

Comparison of the thermal behavior and conformational changes in partially and fully hydrated dipalmitoylphosphatidylcholine systems

Petros Chatzigeorgiou¹ · Athinaida Mourelatou² · Evangelos Pollatos² ·
Dimitra Margari³ · Nikolaos Zogzas⁴ · Kyriakos Viras¹ · Thomas Mavromoustakos^{5,6} ·
Charis E. Semidalas³ 

Received: 21 February 2017 / Accepted: 28 July 2017 / Published online: 7 August 2017
© Akadémiai Kiadó, Budapest, Hungary 2017

Abstract The temperature dependence of conformational changes for partially and fully hydrated DPPC systems through two physicochemical techniques, namely DSC and Raman spectroscopy, is studied. DSC experiments have shown a different thermal behavior between the two considered systems, indicating the effective role of water in the thermal behavior. A temperature resolution of inter- and intramolecular interactions during the main melting phase transition was achieved by using three different Raman intensity ratios, which confirm that the main phase transition represents a two-stage transition. Van't Hoff plots for the C–C, C–H, C=O and C₄N⁺ stretching modes, in a temperature range just below the main transition temperature, have been used to compare the thermodynamic

parameters extracted by the two physicochemical techniques. The significance of these results can be summarized as follows: (a) DSC and Raman spectroscopy have shown complementary results indicating that DPPC exists in partially or fully hydrated states; (b) thermodynamic parameters ΔH and ΔS calculated in both techniques for the two different hydration states of DPPC were in harmony; (c) water more significantly affects the thermal and dynamic properties of fully hydrated DPPC bilayers than of the partially hydrated DPPC; and (d) water disturbs the head-group packing, the alkyl chains interactions and the mesophase region. It appears that the amount of water plays a vital role in the bilayer structure. As more and more extensive studies appear in the literature on biomolecules or drug membrane interactions, this information will be valuable in understanding the role of water in these interactions.

✉ Charis E. Semidalas
chsemid@teiath.gr

¹ Department of Chemistry, Laboratory of Physical Chemistry, National and Kapodistrian University of Athens, Panepistimiopolis, 15771 Athens, Greece

² Department of Food Technology, Technological Educational Institute of Ionian Islands, Vergotis Avenue, 28100 Argostoli, Kefalonia, Greece

³ Department of Food Technology, Laboratory of Organic Chemistry, Technological Educational Institute of Athens, 12210 Egaleo, Greece

⁴ Department of Food Technology, Laboratory of Food Engineering, Technological Educational Institute of Athens, 12210 Egaleo, Greece

⁵ Department of Chemistry, Laboratory of Organic Chemistry, National and Kapodistrian University of Athens, Panepistimiopolis, 15771 Athens, Greece

⁶ Department of Chemistry, York College and the Graduate Center of the City, University of New York, 94-20 Guy R. Brewer Blvd., Jamaica, NY 11451, USA

Keywords Dipalmitoylphosphatidylcholine · DSC · Raman spectroscopy · van't Hoff plots

Introduction

It is well established in the literature that phospholipids are a major constituent of biological membranes. Therefore, the analysis of their physical properties and conformational changes versus temperature in model membrane systems provides fundamental insights into their physicochemical properties and biological function [1, 2]. The thermal behavior of fully hydrated dispersions of DPPC has been extensively investigated by using a variety of physicochemical techniques, such as infrared spectroscopy, X-ray diffraction, neutron diffraction and NMR spectroscopy [3–8]. It is generally agreed upon, that when DPPC is

hydrated spontaneously forms lipid bilayers and is characterized by three thermal phase transitions at specific temperatures. The sub-transition ($L_C \rightarrow L_{\beta'}$) at 17 °C, the pre-transition ($L_{\beta'} \rightarrow P_{\beta'}$) at 35 °C and the main phase transition ($P_{\beta'} \rightarrow L_{\alpha}$) at 41.2 °C [1, 8–15]. The main phase transition is characterized by lateral expansion and thinning of the bilayer thickness, and it is also accompanied by an alternation in the conformations of alkyl chains from an almost “all-*trans*” assembly to one, in which the *gauche* isomers are predominant [6].

Physical chemists mainly focus on the fully hydrated lipid systems as opposed to the partially hydrated systems because of their occurrence in animal cell membranes and anhydrous DPPC [1, 16–19].

The results of three representative studies of anhydrous DPPC are outlined. O’Leary and Levin [6] applied Raman spectroscopy to study the melting behavior of anhydrous dipalmitoyl phosphatidylcholine bilayers. They observed that at in a range of 100–108 °C a cooperative phase transition occurs in which further lateral expansion of the bilayer is accompanied both by an increased number of *gauche* rotamers within the hydrocarbon chain region and by multiple conformers in both the head-group and glycerol backbone moieties. They also noticed that the melting behavior of anhydrous lipid systems is analogous to the completely hydrated dispersion. Meulendijks et al. [20] applied ^{13}C cross-polarization magic-angle spinning NMR on the chain packing in anhydrous and hydrated DL- and L-dipalmitoylphosphatidylcholine (DPPC). They found different packings between DL- and L-DPPC signifying stereospecific interactions in their behavior toward the uptake of water. Interestingly, L-DPPC did not show any packing changes in the acyl chains when going from the anhydrous state to the hydrated forms. Similar results have been found by Sakurai et al. [21] who reported that electron and X-ray diffraction patterns obtained from single crystals of L-type and DL-type lecithins at low temperatures show that chains are nearly perpendicular to the layer in the DL-type DPPC lipid and tilted with a more complicated packing in L-type DPPC [21].

As with fully hydrated phospholipids, partially hydrated phospholipids undergo directly from gel to the liquid crystalline state. Some mesomorphic phases are encountered before the melting point. Effects of water on membrane systems include the depression of the temperature of the main transition and the structural alternations within the polar head-group and glycerol backbone regions of the membranes [6, 22–24]. The study of phosphatidylcholines (lecithins), with the presence of membrane-active drug molecules, has proved to be a productive approach to understand the structure, organization and interactions of lipid bilayer assemblies [6, 25–38].

In this study, the macroscopic method of differential scanning calorimetry along with microscopic Raman spectroscopy is applied to investigate the conformational changes that occur in partially and fully hydrated DPPC. The experimental temperature range varies depending on the temperature in which the phase transitions were observed. These two lipid systems are compared using van’t Hoff plots.

Our research program aims to understand the effect of water in simple phospholipids and more complicated systems (i.e., mixtures of phospholipids containing cholesterol) as well as systems containing bioactive compounds (i.e., drugs).

Materials

DPPC was obtained from Avanti Polar Lipids Inc. (Alabaster, AL, USA); the organic solvents, chloroform (CHCl_3) and methanol (CH_3OH), were of spectroscopic grade and purchased from Sigma-Aldrich (St. Louis, MO).

Differential scanning calorimetry

An amount of 110 mg of DPPC was dissolved in chloroform. The solvent was then evaporated under vacuum (0.1 mm Hg) using a rotary evaporator at 50 °C for 48 h to completely evaporate any residual solvent. A portion of 5 mg of dry material was sealed into stainless steel capsules obtained from Perkin-Elmer Company (Norwalk, Connecticut, USA). No precaution was taken to prevent hydration of this sample, which we therefore called the “partially hydrated sample.” After sealing, gravimetric analysis showed that the sample absorbed 2.1% w/w water (6.1×10^{-3} mmol water and 6.7×10^{-3} mmol phospholipid or water/phospholipid 0.91:1 molar ratio). Another portion of 5 mg of dry material was hydrated with 5 μL of bi-distilled water (50% w/w or 0.28 mmol of water and 7×10^{-3} mmol of phospholipid or water/phospholipid 40:1 molar ratio) and called the “fully hydrated sample.” Partially and fully hydrated samples were treated identically. The hydration of the samples was controlled as the samples were pressed and sealed hermetically.

Thermal scans were obtained on a Perkin-Elmer DSC-4 calorimeter. Prior to scanning, the samples were held above their phase transition temperature for 15 min to ensure equilibration. All samples were scanned at least three times until identical DSC curves were obtained using a scanning rate of $2.5 \text{ }^\circ\text{C min}^{-1}$. The temperature scale of the calorimeter was calibrated using indium ($T_m = 156.6 \text{ }^\circ\text{C}$) as the standard reference sample.

Raman spectroscopy

An amount of 50 mg of partially hydrated and 50 mg of fully hydrated samples was used for Raman spectroscopy experiments. The two samples were hermetically sealed in appropriate cuvettes.

For Raman spectroscopy, a Perkin-Elmer (Norwalk, Connecticut, USA) GX Fourier transform spectrometer was used, equipped with a diode-pumped Nd: YAG laser exciting at 1064 nm. The scattered radiation was collected at an angle of 180° to the incident beam. Spectra were recorded at a laser power of 400 mW with a resolution of 2 cm⁻¹. To obtain a good signal-to-noise ratio, 2000 scans were co-added for each spectrum. A temperature controller system from Ventacon (CAL 3300, Ventacon Ltd, Winchester UK) was used to obtain spectra at different temperatures with a temperature stability of ±0.5 °C. The intensity of a Raman band was observed over a period of time to ensure equilibration of the sample at the given temperature. Analysis of the spectra was carried out using Spectrum Software version No. 3.02.01 (Perkin-Elmer, Norwalk, Connecticut, USA). Raman spectra were obtained in the frequency region of 100–3500 cm⁻¹.

Results and discussion

Differential scanning calorimetry

Differential scanning calorimetry is a well-established method used to monitor lipid phase transitions. By measuring the change in enthalpy of lipid samples as the temperature is varied, phase transitions can be detected. The thermal properties of partially hydrated DPPC derived after removal of the chloroform solvent have been examined at the temperature range of 0–100 °C, with a scanning rate of 2.5 °C min⁻¹. The obtained results by the repeated heating and cooling treatments are shown in Fig. 1a–c. Figure 1a shows the first heating of the sample in which two different phase transitions are observed. The first one is a metastable endothermic transition, which disappeared in the second heating process (Fig. 1c). This peak was observed at $T_{\text{onset}} = 22$ °C with $\Delta H = 1.12 \pm 0.22$ kJ mol⁻¹.

Additionally, the second endothermic phase transition, called main transition, corresponds to the melting of the partially hydrated DPPC bilayers. The temperature for this double-peak melting transition is observed at $T_{\text{m,onset}} = 63.9$ °C ($T_{\text{m}} = 68.4$ °C) giving a $\Delta H = 45.23 \pm 3.67$ kJ mol⁻¹ and $\Delta S = 0.134 \pm 0.011$ kJ mol⁻¹ K⁻¹. The first melting of partially hydrated DPPC bilayers is highly endothermic, but the second melting exhibits a smaller enthalpy of 35.63 ± 2.48 kJ mol⁻¹ and a $\Delta S = 0.106 \pm 0.010$ kJ mol⁻¹ K⁻¹. This observation

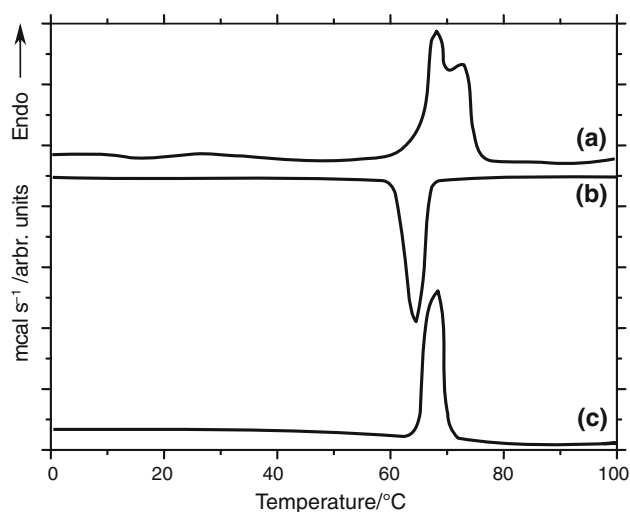


Fig. 1 DSC curves for partially hydrated DPPC: *a* first melting treatment; *b* first cooling treatment; and *c* second melting process

reveals that when the partially hydrated sample melts for the first time, conformational changes occur in acyl chains, polar head groups and the glycerol backbone. In contrast, acyl chain isomerization occurs during the second melting of the sample as cooling does not restore the initial head-group or the glycerol backbone conformations. The thermal scan of the second melted sample which remains constant upon further thermal scans reveals that its hydration is indeed 2.1 mass% if it is compared with literature reported data [39].

The peak at the main phase transition shows a heterogeneous lipid bilayer where the water is associated with a different degree in the lipid bilayer [40].

Figure 2a–c shows the heating–cooling–heating cycle of spontaneously formed fully hydrated DPPC bilayers, at the

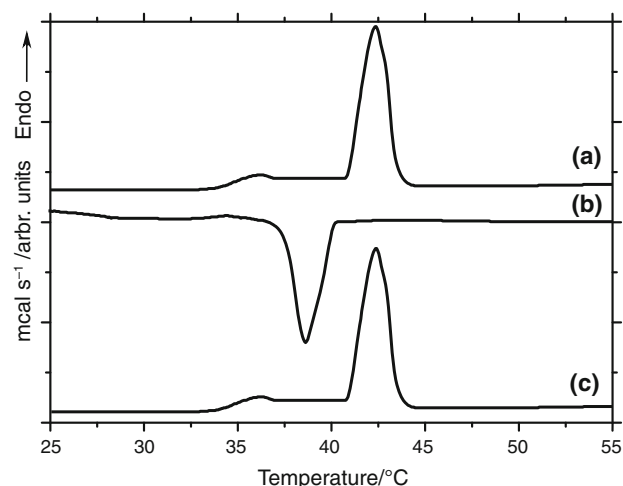


Fig. 2 DSC curves for fully hydrated DPPC bilayers: *a* first heating treatment; *b* first cooling treatment; and *c* second heating process

temperature range of 25–55 °C. In the heating cycle, two phase transitions can occur (Fig. 2a). The first endothermic peak, called pre-transition, is obtained at $T_{p,\text{onset}} = 34.3$ °C ($T_p = 36.0$ °C) giving a $\Delta H = 1.21 \pm 0.09$ kJ mol⁻¹ and $\Delta S = 0.004 \pm 0.001$ kJ mol⁻¹ K⁻¹ and corresponds to a transition from the gel phase $L_{\beta'}$ to the ripple phase $P_{\beta'}$. The second one, called the main transition, is observed at $T_{m,\text{onset}} = 40.9$ °C ($T_m = 42.2$ °C) giving an increment of $\Delta H = 36.00 \pm 2.25$ kJ mol⁻¹ and $\Delta S = 0.088 \pm 0.009$ kJ mol⁻¹ K⁻¹ and corresponds to a transition from the ripple phase $P_{\beta'}$ to the liquid crystalline phase L_{α} . Rappolt and Rapp using X-ray diffraction on multilamellar vesicles of DPPC dispersed in excess water showed that ripple phase (short ripple) is stable upon heating from gel phase but metastable upon cooling from liquid crystalline phase (short and long ripples). $L_{\beta'}$ phase does not readily form in cooling direction. In fact, it takes several hours until the lamellar stacking order is fully achieved [41]. Katsaras and his collaborators suggested a kinetic mechanism, involving loss of water, that promotes formation of the metastable long ripple phase for special thermal protocols [42].

In the vicinity of the $L_{\alpha} \rightarrow P_{\beta'}$ transition of DMPC multibilayers, the thickness of water layer (*dw*) experiences a sudden expansion of about 1.7 Å. In this anomalous expansion, the hydrophobic and head group do not participate [43–45]. Jørgensen using high-sensitivity DSC observed the existence of a sub-main transition in multilamellar bilayers composed of long-chain saturated diacylphosphatidylcholine bilayers. This highly cooperative sub-main transition takes place over a narrow temperature range between the well-known pre-transition and main transition [46].

The temperatures of the transitions have small differences compared with those of heating scanning, caused by the phenomenon of supercooling [47]. The accurate values of these transitions are 33.9 and 39.8 °C, respectively.

In both samples, a significant thermal intrinsic hysteresis is observed. This hysteresis is well established in the literature and attributed to the used scanning rate of 2.5 °C min⁻¹ [48].

Raman spectroscopy

Raman spectroscopy was used to study the conformational changes of partially and fully hydrated dipalmitoylphosphatidylcholine at a temperature range of -120 to 100 °C for partially hydrated and 25–50 °C for fully hydrated DPPC bilayers. This broad temperature range, beyond biological interest, was selected for the detailed study of the observed conformational changes and for the more accurate calculation of the van't Hoff plots. The bands

observed in the spectral region of 100–3500 cm⁻¹ are well established in the literature (corresponding references are given in the discussion of various spectra regions). Representative observed Raman frequencies of partially and fully hydrated DPPC bilayers at 25 °C are given in Table 1. Detailed analysis for the various spectra regions of the obtained Raman spectra at different temperatures is presented. Interfacial regions covering the carbonyl (C=O) stretching mode (1600–1800 cm⁻¹) are analyzed in detail by Bush et al. [22] and Blume et al. [49]. Thus, for this region the discussion will be limited to van't Hoff plots.

700–1000 cm⁻¹

This spectral region includes bands that provide information about polar head group and aliphatic chains. The bands observed at 716 and 962 cm⁻¹ correspond to the symmetric and asymmetric C–N choline stretching modes, respectively, while the band at 888 cm⁻¹ corresponds to the rocking terminal methyl group, which is characteristic of *trans* conformation. The methyl end rocking band is a localized vibration; frequencies of these vibrations are dependent only on local conformation and, as opposed to non-localized modes, tend to be independent of both chain length and the conformation of the rest of the molecule. On the other hand, bands at lower frequencies in the region

Table 1 Observed Raman band frequencies of partially and fully hydrated DPPC bilayers at 25 °C

Partially hydrated DPPC frequency/cm ⁻¹	Fully hydrated DPPC frequency/cm ⁻¹	Assignment
716	716	C–N symmetric stretching
835–875	835–875	CH ₃ deformation of <i>gauche</i> conformers
888	887	CH ₃ rocking of <i>trans</i> conformers
962	960	C–N asymmetric stretching
1060	1062	C–C stretching of <i>trans</i> conformers
1100	1094	C–C stretching of <i>gauche</i> conformers
1127	1128	C–C stretching of <i>trans</i> conformers
1294	1294	CH ₂ twisting
1436	1437	CH ₂ scissoring
1456	1455	CH ₃ asymmetric bending
1724	1725	C=O stretching of <i>sn</i> – 2 chain
1740	1740	C=O stretching of <i>sn</i> – 1 chain
2845	2847	CH ₂ symmetric stretching
2881	2880	CH ₂ asymmetric stretching
2936	2937	CH ₃ symmetric stretching

835–875 cm^{-1} are assigned to methyl end *gauche* conformations [6, 24, 34, 50–56].

As the temperature is raised (Fig. 3a), the band corresponding to the C–N symmetric stretching mode shifts from 716 to 712 cm^{-1} . The shift of the band indicates that interactions between polar head groups are modified significantly. The intensity of the rocking mode at 888 cm^{-1} decreases dramatically and broadens with increase in temperature, until it disappears. Meanwhile, the intensity of the bands at 835–875 cm^{-1} increases rapidly showing an augmentation of the presence of *gauche* conformation. Cooling of the sample did not restore the frequencies and intensities of choline bands, indicating that the change of conformations of choline head groups is irreversible.

For fully hydrated DPPC (Fig. 3b), the band of the C–N symmetric stretching modes shifts from 716 to 713 cm^{-1} as the temperature is increased. This is virtually the same shift as is observed for the partially hydrated DPPC sample. Cooling of the sample restores the frequency and the intensity of the bands in this spectral region, which means that the polar head groups return to their initial structure.

The addition of water in DPPC molecules induces the reversible pre-transition phase change either by exerting electrostatic forces or by the creation of hydrogen bonds between choline head groups and water molecules. The pre-transition ($L_{\beta'} \rightarrow P_{\beta'}$) peak is linked to a change of polar head-group organization that accompanies a change of tilt of the lipid chains from a condition of being tilted to the plane of the lamellae ($L_{\beta'}$) to the vertical condition and to the formation of ripples on the membrane surface ($P_{\beta'}$) [57, 58]. In the partially hydrated sample, aliphatic chains are not tilted (L_{β}) at temperatures below the melting point.

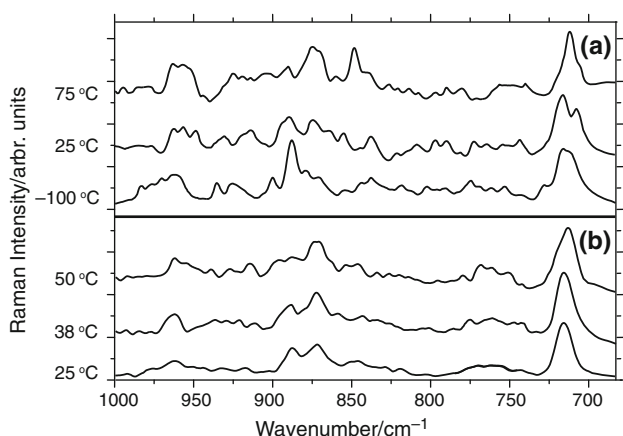


Fig. 3 Normalized Raman spectra at three different selected temperatures in spectral region 700–1000 cm^{-1} of **a** partially hydrated and **b** fully hydrated DPPC bilayers

1000–1200 cm^{-1}

Three major bands that reflect the C–C stretching of the hydrocarbon chains are observed in this spectral region. The bands approximately at 1060 and 1130 cm^{-1} correspond to the C–C stretching mode of *trans* rotamers, while the band approximately at 1090 cm^{-1} corresponds to the C–C stretching mode of *gauche* conformers [6, 15, 52, 59–61]. In the partially hydrated DPPC sample, the presence of the latter band at low temperatures demonstrates that the aliphatic chains are never “all-*trans*,” but they possess some portion of *gauche* rotamers that are anticipated to be at the most flexible region. Figure 4a shows normalized Raman spectra in the examined spectral region at three different temperatures, covering the temperature range previously described. Increasing temperature causes a shift of the frequency of the observed bands. The band assigned to C–C stretching of *gauche* conformers shifts from 1100 to 1095 cm^{-1} and broadens toward lower wave numbers, while the band assigned to C–C stretching of *trans* conformers at 1127 cm^{-1} shifts to 1124 cm^{-1} . These results indicate that the phase of partially hydrated DPPC, after the main transition, has a large amount of *gauche* conformers.

In the case of fully hydrated DPPC molecules (Fig. 4b), the bands that occur in this spectral region have almost the same behavior as in the partially hydrated sample. The *trans* C–C and the *gauche* C–C stretching modes undergo a shift to lower frequencies at about 4 and 8 cm^{-1} , respectively. These greater shifts compared with those of the partially hydrated sample indicate that after the main transition temperature in fully hydrated DPPC bilayers there is greater chain mobility and a larger amount of *gauche* conformers. The same qualitative behavior of the alkyl chains can be understood because the presence of the

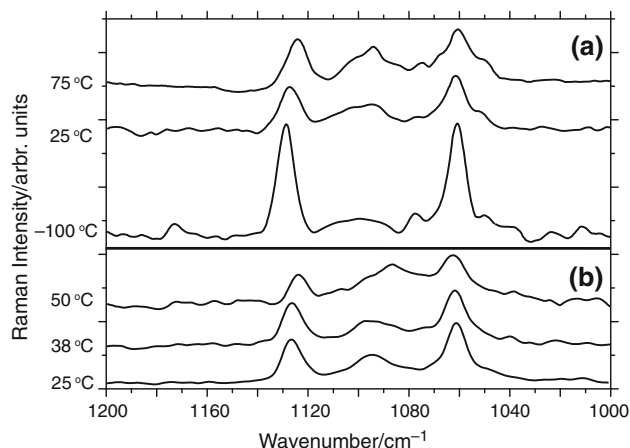


Fig. 4 Normalized Raman spectra at three different selected temperatures in spectral region 1000–1200 cm^{-1} of **a** partially hydrated and **b** fully hydrated DPPC bilayers

water molecules is predominantly in the polar and mesophase regions and does not significantly influence the aliphatic alkyl chain region.

The *gauche/trans* I_{1090}/I_{1130} peak height Raman intensity ratio in the C–C stretching region provides a direct measurement of intrachain disorder and *gauche* population [15, 52, 58, 59]. The value of this ratio increases dramatically near the melting point temperature of the samples. This observation means that the *gauche* population of the hydrocarbon chain increases with higher temperature. The temperature, $T_{m, \text{onset}}$, derived from the temperature profiles fit to the data, is approximately 62.7 ± 0.4 °C for partially hydrated DPPC (Fig. 5a) and 41.6 ± 0.2 °C for fully hydrated DPPC bilayers (Fig. 5b). By comparing the values of the ratio after the melting point, it can be concluded that in the fully hydrated sample there is a larger amount of *gauche* conformers, which suggests the greater fluidity of bilayers in the fully hydrated than in the partially hydrated sample. The midpoints of the sigmoidal curves are in good agreement with $T_{m, \text{onset}}$ calculated by DSC experiments. These results show that although it is well known that water itself is localized mainly in the polar region, a small amount must penetrate into the alkyl chain, which increases the *gauche/trans* isomerization ratio. In addition, its presence in the polar region appears to “loosen” the packing and leads to a lower $T_{m, \text{onset}}$.

1250–1500 cm^{-1}

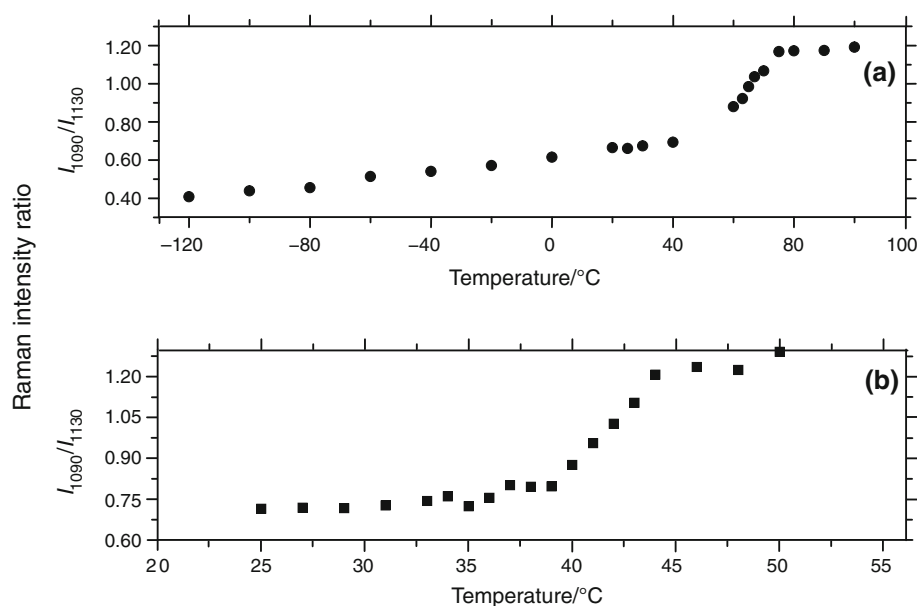
The CH_2 twisting band at 1294 cm^{-1} is superimposed on various modes including the methylene wagging and the CH_2 deformation that are mostly indicative of the

gauche/trans ratio in the acyl chains [6, 15, 62]. In pure alkanes, the asymmetry and width of the CH_2 band have been shown to augment following the raise in temperature, due to the increased freedom of twisting motion that accompanies *gauche* defects [6, 15, 62]. In the studied samples, it is observed that the band at 1294 cm^{-1} decreases in intensity, broadens, becomes more asymmetric and shifts to 1297 cm^{-1} for the partially hydrated sample and to 1299 cm^{-1} for the fully hydrated sample with increasing temperature. This result indicates a decoupling of the acyl chains and disorder in the fully and partially hydrated bilayers. The greater disorder in fully hydrated bilayers corresponds to greater mobility and fluidity of the aliphatic chains of DPPC molecules, a result which is in agreement with those obtained the previous spectral area.

This region also contains several overlapping modes, but the strongest signals come from methylene scissoring at 1436 cm^{-1} and the asymmetric methyl bending at 1456 cm^{-1} [15, 62]. It has been reported that in pure alkanes, a raise in the peak height intensity ratio of the asymmetric methyl bend, compared with that of methylene scissoring, reveals increased intramolecular freedom of motion and chain decoupling, as the temperature is increased [62]. The studied samples seem to follow the same pattern. As the temperature is raised (Fig. 6a), both peaks shift to lower wave numbers, $1437\text{--}1432$ and $1465\text{--}1456 \text{ cm}^{-1}$, respectively, indicating that samples undergo a transition from a quasi-hexagonal to a liquid crystalline state.

The position and the shift of the observed bands in this area can be useful for measuring the *gauche/trans*

Fig. 5 Temperature dependence of peak height Raman intensity ratio I_{1090}/I_{1130} in **a** partially hydrated DPPC and **b** fully hydrated DPPC bilayers



isomerization of the samples (band at 1294 cm^{-1}) and intramolecular freedom of motion and chain decoupling (bands at 1436 and 1456 cm^{-1}). In fully hydrated DPPC bilayers, a greater shift of the band at 1294 cm^{-1} is observed (Fig. 6b). This reveals that the fully hydrated sample has an increased number of *gauche* conformers than the partially hydrated sample. This is confirmed by the fact that the peaks height intensity of the bands at 1436 and 1456 cm^{-1} are almost the same and there is no significant shift of the bands with temperature.

2800–3000 cm^{-1}

Significant changes in the C–H spectral region occur before and during the main phase transition (Fig. 7a, b). The bands at 2844 and 2880 cm^{-1} correspond to C–H symmetric and asymmetric stretching modes of the methylene group, and the band at 2935 cm^{-1} is assigned to the C–H symmetric stretching mode of the methyl terminal group of hydrocarbon chains, respectively [15, 34, 53, 55, 63, 64]. The frequencies of methylene stretching modes represent the level of conformational order and inter-chain coupling in the lipid chains. By increasing the temperature, these bands shift to higher frequencies, signifying chain decoupling. In partially hydrated DPPC (Fig. 7a), the bands which correspond to methylene symmetric and asymmetric stretching modes shift at about 2 and 3 cm^{-1} , respectively, while the band attributed to methyl terminal symmetric stretching mode shift at about 5 cm^{-1} . In the fully hydrated sample, the band at 2880 cm^{-1} represents a higher shift of 5 cm^{-1} .

Moreover, in this region the Raman intensity ratios I_{2840}/I_{2880} and I_{2935}/I_{2880} can be calculated and information about the molecular interactions in the samples can be obtained. The

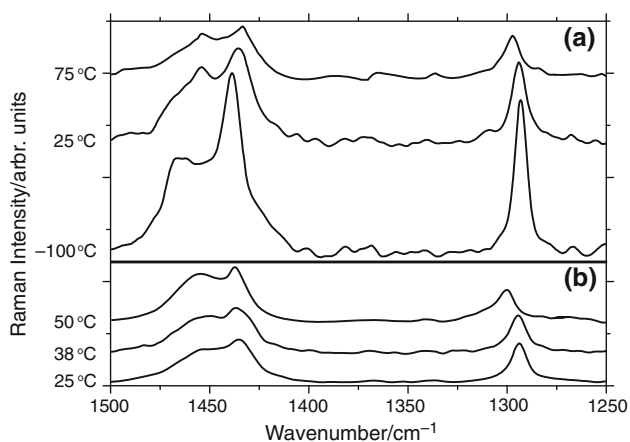


Fig. 6 Normalized Raman spectra at three different selected temperatures in spectral region $1250\text{--}1500\text{ cm}^{-1}$ of **a** partially hydrated DPPC and **b** fully hydrated DPPC bilayers

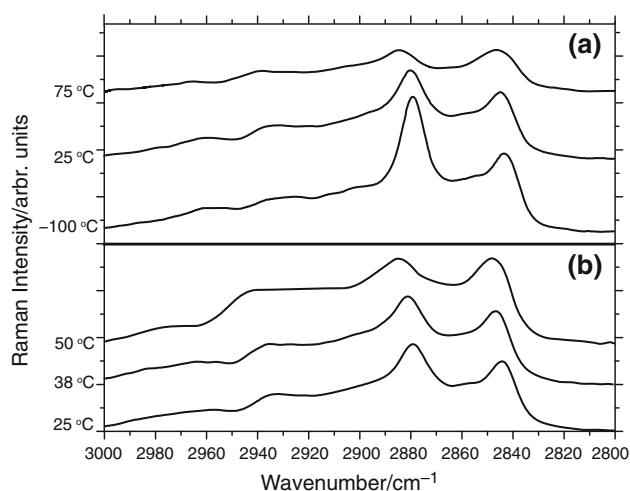


Fig. 7 Normalized Raman spectra at three different selected temperatures in spectral region $2800\text{--}3000\text{ cm}^{-1}$ of **a** partially hydrated DPPC and **b** fully hydrated DPPC bilayers

I_{2840}/I_{2880} ratio provides information about predominantly lipid inter-chain packing behavior, while the I_{2935}/I_{2880} ratio contains information reflecting both inter- and intrachain order/disorder characteristics [6, 15, 34, 55, 63, 65, 66]. The temperatures derived from the temperature profile are approximately $64.4 \pm 0.5\text{ }^\circ\text{C}$ for inter-chain interaction and $62.5 \pm 0.4\text{ }^\circ\text{C}$ for both inter- and intrachain interaction in the case of partially hydrated DPPC (Figs. 8a, 9a) and $41.4 \pm 0.2\text{ }^\circ\text{C}$ for both ratios in the hydrated DPPC bilayers sample (Figs. 8b, 9b). Table 2 summarizes the main Raman results.

Comparison between the phase transition temperatures revealed by Raman spectroscopy with those obtained by DSC shows that these two techniques are in good agreement (RMSD = $0.7\text{ }^\circ\text{C}$).

Van't Hoff plots

The gradual randomization of conformational changes in partially hydrated DPPC at temperatures $60\text{--}69$ and $35\text{--}41\text{ }^\circ\text{C}$ in fully hydrated DPPC bilayers is monitored through Raman spectroscopy by examination of the intensities in various regions in an attempt to calculate the ΔH requirements for the main transition. The acyl linkages and the hydrocarbon chains are studied in the vicinity of T_m to characterize the changes observed at the head group of each sample. In order to compare the melting properties of the lipophilic part, the interface and the head group of the sample, Raman C–H stretching bands are used for monitoring the hydrocarbon chain conformational and lateral inter-chain interactions, the hydrocarbon chain C–C stretching modes for monitoring the *trans*–*gauche* isomerization, the C=O stretching for

Fig. 8 Temperature dependence of peak height Raman intensity ratio I_{2840}/I_{2880} for **a** partially hydrated DPPC sample and **b** fully hydrated DPPC bilayers

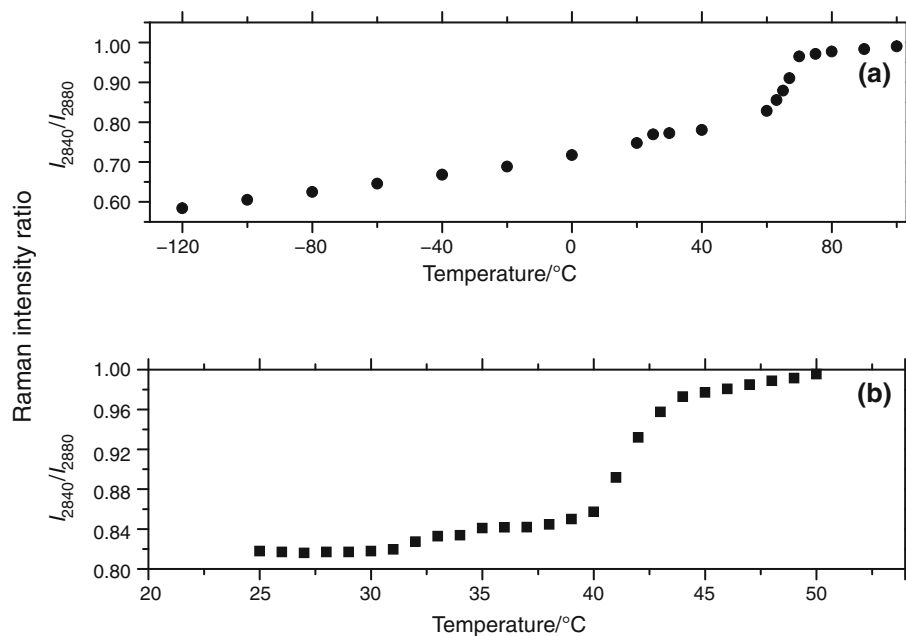
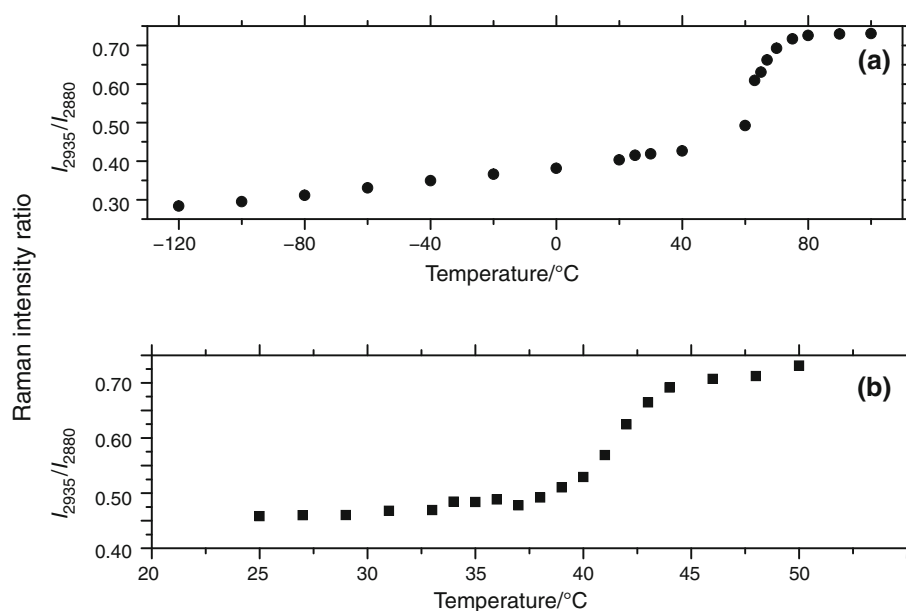


Fig. 9 Temperature dependence of peak height Raman intensity ratio I_{2935}/I_{2880} for **a** partially hydrated sample and **b** fully hydrated DPPC bilayers



motional freedom at the interface and the choline symmetric stretching C–N for head-group electrostatic interactions and motional freedom.

The asymmetric stretching mode of C–H at 2880 cm^{-1} is sensitive to inter-chain and intrachain interactions. It has been noticed that the peak height Raman ratio I_{2840}/I_{2880} decreases gradually below the main transition. For monitoring the changes expressed by this ratio (r), a fractional-

order parameter, θ_{CH} , is used for the hydrocarbon chains. θ_{CH} parameter is given by the equation

$$\theta_{\text{CH}} = \frac{r_t - r}{r_t - r_g} \quad (1)$$

[52]. The values of r_t and r_g were approximated by values obtained experimentally from spectra of partially hydrated DPPC at a minimum ($-120\text{ }^\circ\text{C}$) and maximum ($100\text{ }^\circ\text{C}$)

Table 2 Most important modifications in frequencies and intensities versus temperature increase in partially and fully hydrated DPPC bilayers

Frequency/ cm ⁻¹	Temperature increase/°C
716	3–4 cm ⁻¹ shift to lower wave numbers due to the modification of polar head-group interactions
835–875	Intensity increase due to augmentation of the presence of <i>gauche</i> conformation
888	Decrease in intensity until it disappears
1100	4–8 cm ⁻¹ shift to lower wave numbers due to greater chain mobility and the presence of larger amount of <i>gauche</i> conformers
1127	4–8 cm ⁻¹ shift to lower wave numbers due to greater chain mobility and the presence of larger amount of <i>gauche</i> conformers
1294	Decrease in intensity and 3–5 cm ⁻¹ shift to higher wave numbers due to decoupling of the acyl chains and the disorder in the fully and partially hydrated bilayers
1436	Increase of peak height intensity ratio 1456/1436 due to increasing intramolecular freedom of motion and chain decoupling. 5 cm ⁻¹ shift to lower wave numbers due to transition from a quasi-hexagonal to a liquid crystalline state
1456	9 cm ⁻¹ shift to lower wave numbers due to transition from a quasi-hexagonal to a liquid crystalline state
2845	2 cm ⁻¹ shift to higher wave numbers due to chain decoupling
2881	3–5 cm ⁻¹ shift to higher wave numbers due to chain decoupling
2936	5 cm ⁻¹ shift to higher wave numbers due to chain decoupling

temperature, and r represents the value observed at any other temperature.

The symmetric stretching mode of C–C at 1127 cm⁻¹ is sensitive to the *trans* isomers/conformers, and the symmetric stretching of C–N at 716 cm⁻¹ is used as an internal

standard below the main transition. The θ_{CC} order parameter is given by the equation

$$\theta_{CC} = \frac{I_{1127}}{I_{716}} \left(\frac{I_{1127}}{I_{716}} \right)_t \quad (2)$$

[52], where t is the lowest temperature for the experiment and the side chains are considered to be “all-*trans*.”

For monitoring the changes observed at the acyl linkages, the bands at 1724 and 1740 cm⁻¹ were used, which correspond to non-hydrated and hydrated carbonyl groups [6, 49] at $sn - 1$ or $sn - 2$ positions [22]. The fractional-order parameter for the acyl region is given by the equation

$$\theta_{C=O} = \frac{2 \cdot I_{1724}}{(I_{1724} + I_{1740})} \quad (3)$$

[52], where the band at 1724 cm⁻¹ presents the population of the *trans* conformers and the band at 1740 cm⁻¹ represents the population of the *gauche* conformers.

To determine the enthalpy and entropy requirements of the conformer's isomerization at the lipophilic part, the interface and head-group areas of the sample, the slopes of van't Hoff plots of $\ln \theta / (1 - \theta)$ versus $1/T$ (K⁻¹) were used for the three fractional-order parameters [52]. The enthalpies were calculated from the slopes of the van't Hoff plots, and the entropies during the main phase transitions were calculated from the standard parameters. The obtained results are summarized in Table 3 and are presented in Fig. 10a and b. The changes that occurred at the lipophilic part and the head group presented endothermic behavior, because of the *gauche/trans* isomerization, while the changes at the interface showed exothermic behavior caused by the thinning of the thickness of the interface area in partially hydrated DPPC. By adding the observed values for enthalpy and entropy requirements in partially and fully hydrated samples, it has been concluded that they are in agreement with those obtained by DSC experiment.

Table 3 Enthalpy and entropy requirements for the main phase transition as estimated using van't Hoff plots for the lipophilic part, the interface and the head-group regions of partially and fully hydrated DPPC bilayers

Fractional parameter	$\Delta H/\text{kJ mol}^{-1}$	$\Delta S/\text{kJ mol}^{-1} \text{K}^{-1}$	$\Delta H/\text{kJ mol}^{-1}$	$\Delta S/\text{kJ mol}^{-1} \text{K}^{-1}$
	Partially hydrated DPPC bilayers		Fully hydrated DPPC bilayers	
θ_{CC}	36.35 ± 5.84	0.098 ± 0.017	-28.75 ± 1.41	-0.195 ± 0.005
θ_{CO}	-5.48 ± 0.94	-0.015 ± 0.003	93.95 ± 7.21	0.490 ± 0.023
Θ_{CH}	14.68 ± 0.64	0.044 ± 0.002	-28.75 ± 1.41	-0.195 ± 0.005
Raman total	45.55 ± 5.54	0.127 ± 0.016	36.45 ± 4.39	0.100 ± 0.013
DSC total	45.23 ± 3.67	0.134 ± 0.011	36.00 ± 2.25	0.088 ± 0.009

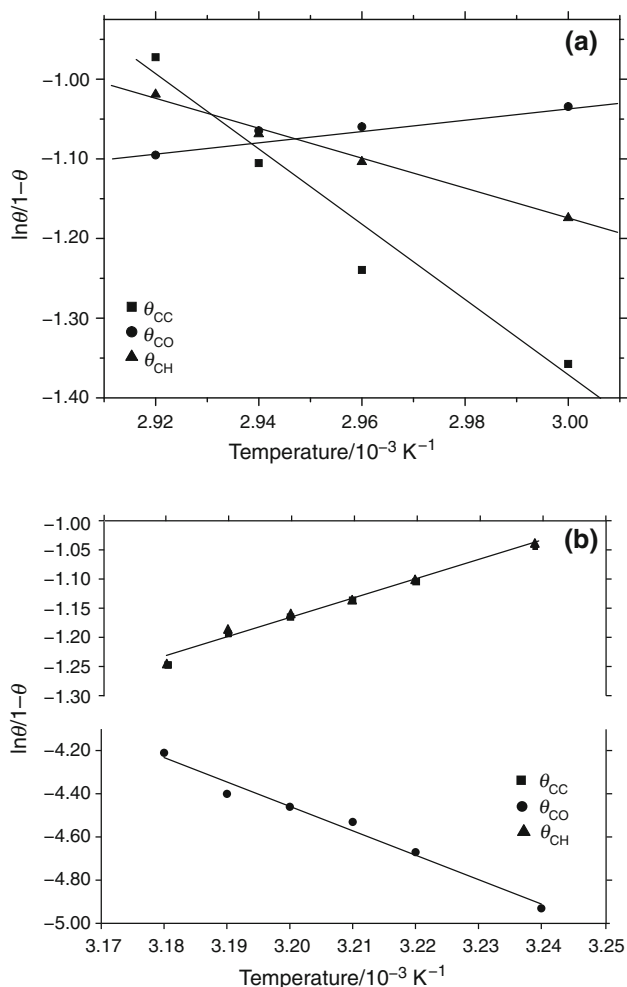


Fig. 10 Van't Hoff plots for three different fractional parameters in **a** partially hydrated and **b** fully hydrated sample

Conclusions

In this study, a physicochemical comparison of the phase transitions of partially and fully hydrated dipalmitoylphosphatidylcholine (DPPC) is presented by using differential scanning calorimetry (DSC) and Raman spectroscopy. This analysis revealed the differences and similarities in conformational changes that are observed in DPPC molecules in the partially and fully hydrated DPPC bilayers.

In the partially hydrated DPPC system, only one phase transition, called the main transition, is observed, at $T_m = 68.4$ °C. The ΔH requirements of the transition depend on the heating history of the sample. This is attributed to the different organization of the polar head groups in DPPC molecules after heating and cooling cycles. In comparison, in the defined fully hydrated samples the polar head groups show a reversible transition, called pre-transition at $T_p = 36.0$ °C and main transition at

$T_m = 42.2$ °C. This observation agrees with the results from Raman spectroscopy, which show that in the partially hydrated DPPC sample, the intensities of the peaks corresponding to polar head groups are not restored in conformation. The pre-transition endothermic peak in the fully hydrated bilayer is associated with a change of polar head-group organization accompanied by change of tilt of the lipid chains from a condition of being tilted to the plane of the lamellae to the vertical condition. The main phase transition is mainly associated with *trans/gauche* isomerization of the alkyl chains.

The peak height Raman intensity ratios I_{1090}/I_{1130} , I_{2840}/I_{2880} and I_{2935}/I_{2880} show that the hydrocarbon chain mobility in the fully hydrated liquid crystalline system is greater than in the partially hydrated liquid crystals. This is because the addition of water molecules increases the area per DPPC molecule and induces increased population of *gauche* conformers. Moreover, the addition of the water decreases the main transition temperature from $T_m = 68.4$ °C to $T_m = 42.2$ °C. This temperature value is the minimum temperature required for water to penetrate between layers of the lipid molecules.

The present results demonstrate that DSC and Raman spectroscopy provide thermodynamic parameters and complementary results in partially and fully hydrated lipids bilayers. For example, the temperature $T_{m,onset}$ observed by DSC was in good agreement with the values obtained by the temperature profile of peak height Raman intensity ratios. The enthalpy and entropy requirements from DSC experiments can also be calculated by figuring out van't Hoff plots. The next step is to study the application of van't Hoff plots for fully hydrated mixtures of DPPC bilayers with inserted different concentrations of biological active compounds such as phenolic compounds, amino acids, cholesterol, peptides and drugs [26, 29, 67–75].

Acknowledgements This research was co-financed by the European Union (European Social Fund—ESF) and Greek National funds through the Operational Program “Education and Lifelong Learning” of the National Strategic Reference Framework (NSRF)—Research Funding Program: ARCHIMEDES III. Investing in knowledge society through the European Social Fund. The authors would like to acknowledge Ms. Shiri Arnon from UC Santa Barbara for proof-reading the manuscript (Grant No. HTYSBIOP 021215).

References

1. Koynova R, Caffrey M. Phases and phase transitions of the phosphatidylcholines. *Biochim Biophys Acta Rev Biomembr.* 1998;1376:91–145.
2. Koynova R, Caffrey M. An index of lipid phase diagrams. *Chem Phys Lipids.* 2002;115:107–219.
3. Chapman D. Phase transitions and fluidity characteristics of lipids and cell membranes. *Q Rev Biophys.* 1975;8:185–235.

4. Shinitzky M, Barenholz Y. Fluidity parameters of lipid regions determined by fluorescence polarization. *Biochim Biophys Acta Netherlands*. 1978;515:367–94.
5. Israelachvili JN, Marčelja S, Horn RG. Physical principles of membrane organization. *Q Rev Biophys*. 1980;13:121–200.
6. O'Leary TJC, Levin IW. Effects of solvent on biomembrane structure: Raman spectroscopic investigation of dipalmitoylphosphatidylcholine dispersed in N-ethylammonium nitrate. *J Phys Chem*. 1984;88:4074–8.
7. Agelis G, Resvani A, Ntountaniotis D, Chatzigeorgiou P, Koukoulitsa C, Androutsou ME, Plotas P, Matsoukas J, Mavromoustakos T, Čendak T, Ukmar Codec T, Mali G. Interactions of the potent synthetic AT1 antagonist analog BV6 with membrane bilayers and mesoporous silicate matrices. *Biochim Biophys Acta Biomembr*. 2013;1828:1846–55.
8. Zhernenkov M, Bolmatov D, Soloviov D, Zhernenkov K, Toperverg BP, Cunsolo A, Bosak A, Cai YQ. Revealing the mechanism of passive transport in lipid bilayers via phonon-mediated nanometre-scale density fluctuations. *Nat Commun*. 2016;7:11575.
9. Le Bihan T, Pézolet M. Study of the structure and phase behavior of dipalmitoylphosphatidylcholine by infrared spectroscopy: characterization of the pretransition and subtransition. *Chem Phys Lipids*. 1998;94:13–33.
10. Mason JT. Investigation of phase transitions in bilayer membranes. *Methods Enzymol*. 1998;295:468–94.
11. Meyer HW, Semmler K, Rettig W, Pohle W, Ulrich AS, Grage S, Selle C, Quinn PJ. Hydration of DMPC and DPPC at 4 °C produces a novel subgel phase with convex–concave bilayer curvatures. *Chem Phys Lipids*. 2000;105:149–66.
12. Tenchov B, Koynova R, Rapp G. New ordered metastable phases between the gel and subgel phases in hydrated phospholipids. *Biophys J*. 2001;80:1873–90.
13. Kranenburg M, Smit B. Phase behavior of model lipid bilayers. *J Phys Chem B*. 2005;109:6553–63.
14. Mouritsen OG. *Life—as a matter of fat: the emerging science of lipidomics*. New York: Springer; 2005.
15. Fox CB, Uibel RH, Harris JM. Detecting phase transitions in phosphatidylcholine vesicles by Raman microscopy and self-modeling curve resolution. *J Phys Chem B*. 2007;111:11428–36.
16. Kučerka N, Tristram-Nagle S, Nagle JF. Closer look at structure of fully hydrated fluid phase DPPC bilayers. *Biophys J Biophys Soc*. 2006;90:L83–5.
17. Grillo D, Olvera de la Cruz M, Szleifer I. Theoretical studies of the phase behavior of DPPC bilayers in the presence of macroions. *Soft Matter*. 2011;7:4672–9.
18. Prates Ramalho JP, Gkeka P, Sarkisov L. Structure and phase transformations of DPPC lipid bilayers in the presence of nanoparticles: insights from coarse-grained molecular dynamics simulations. *Langmuir*. 2011;27:3723–30.
19. Curtis EM, Hall CK. Molecular dynamics simulations of DPPC bilayers using “LIME”, a new coarse-grained model. *J Phys Chem B*. 2013;117:5019–30.
20. Meulendijks GHWM, De Haan JW, Vos AHJA, de Ven LJM, Buck HM. Carbon-13 cross-polarization magic-angle-spinning NMR study on the chain packing in anhydrous and hydrated DL- and L-dipalmitoylphosphatidylcholine. *J Phys Chem*. 1989;93:3806–9.
21. Sakurai I, Sakurai S, Sakurai T, Seto T, Ikegami A, Iwayanagi S. Electron diffraction study on single crystals of l-type and dl-type lecithins. *Chem Phys Lipids*. 1980;26:41–8.
22. Bush SF, Adams RG, Levin IW. Structural reorganizations in lipid bilayer systems: effect of hydration and sterol addition on Raman spectra of dipalmitoylphosphatidylcholine multilayers. *Biochemistry*. 1980;19:4429–36.
23. Kint S, Wermer PH, Scherer JR. Raman spectra of hydrated phospholipid bilayers. 2. Water and head-group interactions. *J Phys Chem*. 1992;96:446–52.
24. Bicknell-Brown E, Brown KG, Person WB. Configuration-dependent Raman bands of phospholipid surfaces: 2—Head group and acyl stretching modes in the 800–900 cm⁻¹ region. *J Raman Spectrosc*. 1981;11:356–62.
25. Hwang SB, Shen TY. Membrane effects of antiinflammatory agents. 2. Interaction of nonsteroidal antiinflammatory drugs with liposome and purple membranes. *J Med Chem*. 1981;24:1202–11.
26. Mavromoustakos T, Daliani I. Effects of cannabinoids in membrane bilayers containing cholesterol. *Biochim Biophys Acta Biomembr*. 1999;1420:252–65.
27. Lygde H, Moe G, Holmsen H. Interaction of ibuprofen with eukaryotic membrane lipids. *Acta Odontol Scand*. 2003;61:303–9.
28. Kyrikou I, Hadjikakou SK, Kovala-Demertzi D, Viras K, Mavromoustakos T. Effects of non-steroid anti-inflammatory drugs in membrane bilayers. *Chem Phys Lipids*. 2004;132:157–69.
29. Kyrikou I, Daliani I, Mavromoustakos T, Maswadeh H, Demetzos C, Hatziantoniou S, Giatrellis S, Nounesis G. The modulation of thermal properties of vinblastine by cholesterol in membrane bilayers. *Biochim Biophys Acta Biomembr*. 2004;1661:1–8.
30. Procházka M, Štěpánek J, Turpin P-Y. Interaction of phospholipid dispersions with water-soluble porphyrins as monitored by their Raman temperature profiles. *Chem Phys Lipids*. 2004;132:145–56.
31. Bardonnat PL, Faivre V, Pirot F, Boullanger P, Falson F. Cholesteryl oligoethyleneglycol glycosides: fluidizing effect of their embedment into phospholipid bilayers. *Biochem Biophys Res Commun*. 2005;329:1186–92.
32. Severcan F, Sahin I, Kazanci N. Melatonin strongly interacts with zwitterionic model membranes—evidence from Fourier transform infrared spectroscopy and differential scanning calorimetry. *Biochim Biophys Acta Biomembr*. 2005;1668:215–22.
33. Koukoulitsa C, Kyrikou I, Demetzos C, Mavromoustakos T. The role of the anticancer drug vinorelbine in lipid bilayers using differential scanning calorimetry and molecular modeling. *Chem Phys Lipids*. 2006;144:85–95.
34. Kyrikou I, Benetis NP, Chatzigeorgiou P, Zervou M, Viras K, Poulos C, Mavromoustakos T. Interactions of the dipeptide paralyisin β-Ala-Tyr and the amino acid Glu with phospholipid bilayers. *Biochim Biophys Acta Biomembr*. 2008;1778:113–24.
35. Ntountaniotis D, Kellici T, Tzakos A, Kolokotroni P, Tselios T, Becker-Baldus J, Glaubitz C, Lin S, Makriyannis A, Mavromoustakos T. The application of solid-state NMR spectroscopy to study candesartan cilexetil (TCV-116) membrane interactions. Comparative study with the AT1R antagonist drug olmesartan. *Biochim Biophys Acta Biomembr*. 2014;1838:2439–50.
36. Fotakis C, Megariotis G, Christodouleas D, Kritsi E, Zoumpoulakis P, Ntountaniotis D, Zervou M, Potamitis C, Hodzic A, Pabst G, Rappolt M, Mali G, Baldus J, Glaubitz C, Papadopoulos MG, Afantitis A, Melagraki G, Mavromoustakos T. Comparative study of the AT1 receptor prodrug antagonist candesartan cilexetil with other sartans on the interactions with membrane bilayers. *Biochim Biophys Acta Biomembr*. 2012;1818:3107–20.
37. Di Foggia M, Bonora S, Tinti ATV. DSC and Raman study of DMPC liposomes in presence of Ibuprofen at different pH. *J Therm Anal Calorim*. 2017;127:1407–17.
38. Rakic V, Ota A, Sokolovic D, Ulrich NP. Interactions of cyanidin and cyanidin 3-O-β-glucopyranoside with model lipid membranes. *J Therm Anal Calorim*. 2017;127:1467–77.
39. Kodama M, Kuwabara M, Seki S. Successive phase-transition phenomena and phase diagram of the phosphatidylcholine-water system as revealed by differential scanning calorimetry. *BBA Biomembr*. 1982;689:567–70.

40. Yeagle P. The structure of biological membranes. 2nd ed. Boca Raton: CRC Press; 2004.
41. Rappolt M, Rapp G. Structure of the stable and metastable ripple phase of dipalmitoylphosphatidylcholine. *Eur Biophys J*. 1996;24:381–6.
42. Katsaras J, Tristram-Nagle S, Liu Y, Headrick RL, Fontes E, Mason PC, Nagle JF. Clarification of the ripple phase of lecithin bilayers using fully hydrated, aligned samples. *Phys Rev E Stat Phys Plasmas Fluids Relat Interdiscip Topics*. 2000;61:5668–77.
43. Pabst G, Amenitsch H, Kharakoz DP, Laggner P, Rappolt M. Structure and fluctuations of phosphatidylcholines in the vicinity of the main phase transition. *Phys Rev E Stat Nonlinear: Soft Matter Phys*; 2004. p. 70.
44. Mason PC, Nagle JF, Epanand RM, Katsaras J. Anomalous swelling in phospholipid bilayers is not coupled to the formation of a ripple phase. *Phys Rev E*. 2001;63:30902.
45. Pabst G, Katsaras J, Raghunathan VA, Rappolt M. Structure and interactions in the anomalous swelling regime of phospholipid bilayers. *Langmuir*. 2003;19:1716–22.
46. Jørgensen K. Calorimetric detection of a sub-main transition in long-chain phosphatidylcholine lipid bilayers. *BBA Biomembr*. 1995;1240:111–4.
47. Wunderlich B. Transitions in one-component systems. Thermal analysis. Boston: Academic Press; 1990. p. 104.
48. Prenner E, Chiu M. Differential scanning calorimetry: an invaluable tool for a detailed thermodynamic characterization of macromolecules and their interactions. *J Pharm Bioallied Sci*. 2011;3:39.
49. Blume A, Huebner W, Messner G. Fourier transform infrared spectroscopy of ¹³C: O labeled phospholipids hydrogen bonding to carbonyl groups. *Biochemistry*. 1988;27:8239–49.
50. Zerbi G, Magni R, Gussoni M, Moritz KH, Bigotto A, Dirlikov S. Molecular mechanics for phase transition and melting of n-alkanes: a spectroscopic study of molecular mobility of solid n-nonadecane. *J Chem Phys*. 1981;75:3175–94.
51. Maroncelli M, Qi S. Nonplanar conformers and the phase behavior of solid n-alkanes. *J Am Chem Soc*. 1982;104:6237–47.
52. Bicknell-Brown E, Brown KG. Raman temperature study of conformational changes in anhydrous dipalmitoylphosphatidylcholine. *Biochim Biophys Acta Biomembr*. 1984;778:317–23.
53. O'Leary TJ, Ross PD, Levin IW. Effects of anesthetic and nonanesthetic steroids on dipalmitoylphosphatidylcholine liposomes: a calorimetric and Raman spectroscopic investigation. *Biochemistry*. 1984;23:4636–41.
54. Maissara M, Devaure J. Raman study of odd-numbered C₁₁–C₂₃ n-alkanes in their high-temperature solid phases. *J Raman Spectrosc*. 1987;18:181–4.
55. Omura Y, Muraishi S. Spectral distortion and sample heating in 1064 nm FT-Raman spectra of aqueous dispersions of dipalmitoylphosphatidylcholine. *Spectrochim Acta Part A Mol Biomol Spectrosc*. 1997;53:1783–94.
56. Lüttschwager NOB, Suhm MA. Stretching and folding of 2-nanometer hydrocarbon rods. *Soft Matter*. 2014;10:4885–901.
57. McIntosh TJ. Differences in hydrocarbon chain tilt between hydrated phosphatidylethanolamine and phosphatidylcholine bilayers. A molecular packing model. *Biophys J*. 1980;29:237–45.
58. Rand RP, Chapman D, Larsson K. Tilted hydrocarbon chains of dipalmitoyl lecithin become perpendicular to the bilayer before melting. *Biophys J U S*. 1975;15:1117–24.
59. Susi H, Byler DM, Damert WC. Raman intensities of carbon-carbon stretching modes in a model membrane. *Chem Phys Lipids*. 1980;27:337–44.
60. Litman BJ, Lewis EN, Levin IW. Packing characteristics of highly unsaturated bilayer lipids: Raman spectroscopic studies of multilamellar phosphatidylcholine dispersions. *Biochemistry*. 1991;30:313–9.
61. Csizsár A, Koglin E, Meier RJ, Klumpp E. The phase transition behavior of 1,2-dipalmitoyl-sn-glycero-3-phosphocholine (DPPC) model membrane influenced by 2,4-dichlorophenol—an FT-Raman spectroscopy study. *Chem Phys Lipids*. 2006;139:115–24.
62. Orendorff CJ, Ducey MW, Pemberton JE. Quantitative correlation of raman spectral indicators in determining conformational order in alkyl chains. *J Phys Chem A*. 2002;106:6991–8.
63. Fox CB, Horton RA, Harris JM. Detection of drug-membrane interactions in individual phospholipid vesicles by confocal Raman microscopy. *Anal Chem*. 2006;78:4918–24.
64. Zheng M, Du W. Phase behavior, conformations, thermodynamic properties, and molecular motion of multicomponent paraffin waxes: a Raman spectroscopy study. *Vib Spectrosc*. 2006;40:219–24.
65. Bunow MR, Levin IW. Comment on the carbon-hydrogen stretching region of vibrational Raman spectra of phospholipids. *Biochim Biophys Acta (BBA)/Lipids Lipid Metab*. 1977;487:388–94.
66. Vincent JS, Levin IW. Interaction of ferricytochrome c with zwitterionic phospholipid bilayers: a Raman spectroscopic study. *Biochemistry*. 1988;27:3438–46.
67. Mavromoustakos T, Yang DP, Charalambous A, Herbet LG, Makriyannis A. Study of the topography of cannabinoids in model membranes using X-ray diffraction. *BBA Biomembr*. 1990;1024:336–44.
68. Yang DP, Mavromoustakos T, Beshah K, Makriyannis A. Amphipathic interactions of cannabinoids with membranes. A comparison between delta 8-THC and its O-methyl analog using differential scanning calorimetry, X-ray diffraction and solid state ²H-NMR. *Biochim Biophys Acta*. 1992;1103:25–36.
69. Mavromoustakos T, Theodoropoulou E, Yang D-P. The use of high-resolution solid-state NMR spectroscopy and differential scanning calorimetry to study interactions of anaesthetic steroids with membrane. *Biochim Biophys Acta Biomembr*. 1997;1328:65–73.
70. Mavromoustakos T, Papahatjis D, Laggner P. Differential membrane fluidization by active and inactive cannabinoid analogues. *Biochim Biophys Acta Biomembr*. 2001;1512:183–90.
71. Maswadeh H, Demetozos C, Daliani I, Kyrikou I, Mavromoustakos T, Tsortos A, Nounesis G. A molecular basis explanation of the dynamic and thermal effects of vinblastine sulfate upon dipalmitoylphosphatidylcholine bilayer membranes. *Biochim Biophys Acta*. 2002;567:49–55.
72. Fotakis C, Gega S, Siapi E, Potamitis C, Viras K, Moutevelis-Minakakis P, Kokotos CG, Durdagi S, Grdadolnik SG, Sartori B, Rappolt M, Mavromoustakos T. Interactions at the bilayer interface and receptor site induced by the novel synthetic pyrrolidinone analog MMK3. *Biochim Biophys Acta Biomembr*. 2010;1798:422–32.
73. Potamitis C, Chatzigeorgiou P, Siapi E, Viras K, Mavromoustakos T, Hodzic A, Pabst G, Cacho-Nerin F, Laggner P, Rappolt M. Interactions of the AT₁ antagonist valsartan with dipalmitoylphosphatidylcholine bilayers. *Biochim. Biophys. Acta Biomembr*. 2011;1808:1753–63.
74. Kellici TF, Ntountaniotis D, Leonis G, Chatziathanasiadou M, Chatzikonstantinou AV, Becker-Baldus J, Glaubitz C, Tzakos AG, Viras K, Chatzigeorgiou P, Tzimas S, Kefala E, Valsami G, Archontaki H, Papadopoulos MG, Mavromoustakos T. Investigation of the interactions of silibinin with 2-hydroxypropyl-beta-cyclodextrin through biophysical techniques and computational methods. *Mol Pharm*. 2015;12:954–65.
75. Sadehpour A, Rappolt M, Ntountaniotis D, Chatzigeorgiou P, Viras K, Megariotis G, Papadopoulos MG, Siapi E, Mali G, Mavromoustakos T. Comparative study of interactions of aliskiren and AT₁ receptor antagonists with lipid bilayers. *Biochim Biophys Acta*. 2015;1848:984–94.